UNSTEADY NAVIER-STOKES COMPUTATIONS OVER AIRFOILS
USING BOTH FIXED AND DYNAMIC MESHES

Christopher L. Rumsey
W. Kyle Anderson
NASA Langley Research Center
Hampton, Virginia

- PURPOSE

- GOVERNING EQUATIONS

- NUMERICAL METHOD

- CONSTANT ANGLE-OF-ATTACK UNSTEADY SOLUTIONS

- FORCED PITCHING SOLUTIONS
    - SINUSOIDAL PITCH
    - CONSTANT-RATE PITCH

- CONCLUSIONS

The purpose of the present investigation is to solve the Navier-Stokes equations for unsteady airfoil flows. Two primary types of unsteady flows are considered. The first is unsteady periodic flow over an airfoil at a fixed angle-of-attack past stall. The second is unsteady flow over an airfoil which is pitching either sinusoidally or with a constant-rate pitch-up motion. For the pitching airfoil solutions, a dynamic mesh is employed in the computations. All results are compared with experiment.

- **NAVIER-STOKES EQUATIONS APPLIED TO UNSTEADY FLOWS ON FIXED MESHES**

- **NAVIER-STOKES EQUATIONS APPLIED TO UNSTEADY FLOWS ON DYNAMIC MESHES**
  - **INCLUDE TIME TERMS IN FLUX VECTORS**
  - **SINUSOIDAL PITCH SOLUTIONS**
  - **CONSTANT-RATE PITCH SOLUTIONS**

- **COMPARISON WITH EXPERIMENT**

The governing equations used in the present analysis are the two-dimensional Reynolds averaged thin-layer Navier-Stokes equations. They are written in generalized coordinates, with the η-coordinate direction along the body and the ζ-coordinate direction normal to the body. Q represents the conserved flow variables. The flux vectors G and H are split according to the method of Van Leer[1], with the extension to dynamic meshes given by Anderson et al[2]. J is the coordinate transformation Jacobian. For an unmoving mesh, η_t and ζ_t are zero.
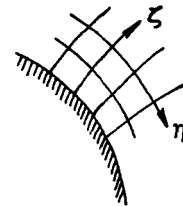
Thin-Layer Navier-Stokes

$$\frac{\partial \hat{Q}}{\partial t} + \frac{\partial \hat{G}}{\partial \eta} + \frac{\partial \hat{H}}{\partial \zeta} = \overline{Re}^{-1} \partial_\zeta [J^{-1}(\zeta_x R + \zeta_y S)]$$

$$\hat{Q} = Q/J$$
$$\hat{G} = (\eta_x G + \eta_y H + \eta_t Q)/J$$
$$\hat{H} = (\zeta_x G + \zeta_y H + \zeta_t Q)/J$$

$$Q = \begin{bmatrix} \rho \\ \rho u \\ \rho v \\ e \end{bmatrix} \qquad G = \begin{bmatrix} \rho u \\ \rho u^2 + p \\ \rho uv \\ u(e + p) \end{bmatrix} \qquad H = \begin{bmatrix} \rho v \\ \rho uv \\ \rho v^2 + p \\ v(e + p) \end{bmatrix}$$

$$R = \begin{bmatrix} 0 \\ \tau_{xx} \\ \tau_{xy} \\ u\tau_{xx} + v\tau_{xy} + \mu Pr^{-1}(\gamma-1)^{-1}\zeta_x(a^2)_\zeta \end{bmatrix} \qquad S = \begin{bmatrix} 0 \\ \tau_{xy} \\ \tau_{yy} \\ u\tau_{xy} + v\tau_{yy} + \mu Pr^{-1}(\gamma-1)^{-1}\zeta_y(a^2)_\zeta \end{bmatrix}$$

378

FLUX SPLITTING

Fluxes are split into a forward and a backward contribution according to the signs of the eigenvalues of the Jacobian matrices, and differenced accordingly. The split-flux differences are implemented as a flux balance across a cell, corresponding to MUSCL (Monotone Upstream-centered Schemes for Conservation Laws)[3] type differencing. For example, the derivative in F at the i node in the figure can be written as $F(Q)_{i+1/2} - F(Q)_{i-1/2}$, where each $F(Q)$ can be split into its forward and backward components F^+ and F^-. State variables on each interface are obtained by interpolation of the conserved variables at the appropriate nodes. Using upwind-biasing, for example, conserved variables at the i-1, i, and i+1 nodes are used to obtain the positive contribution to F(Q) at the i+1/2 interface. The Van Leer splitting has the advantage over more conventional splittings that it is continuously differentiable, and allows shocks to be captured with at most two interior zones.

- Split fluxes into forward and backward contributions
  $$F(Q) = F^+(Q^-) + F^-(Q^+)$$

- Use upwind biased approximation to spatial derivatives

- Van Leer splitting
  - Continuously differentiable
  - Allows shocks to be captured with at most two (usually one) interior zones

i-1/2 i+1/2

i-1   i   i+1
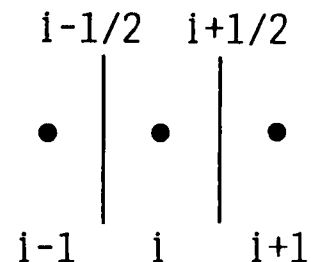
An implicit, upwind-biased, finite-volume scheme is used to numerically solve the thin-layer Navier-Stokes equations. The system of equations is approximately factored and solved in two sweeps. The (+) and (-) superscripts indicate positive and negative flux split quantities. All viscous terms are centrally differenced. The A, B, and M matrices arise from linearizations of the G flux, H flux, and the viscous terms, respectively. The method is second order accurate in space and first order accurate in time. The algebraic eddy viscosity Baldwin-Lomax turbulence model[4] is used for all turbulent flow computations. Boundary conditions are applied explicitly.

Upwind Finite-Volume Approximate-Factorization

$$[\frac{I}{J\Delta t} + \partial_\eta{}^- A^+ + \partial_\eta{}^+ A^-] \Delta Q^* = -RHS$$

$$[\frac{I}{J\Delta t} + \partial_\zeta{}^- B^+ + \partial_\zeta{}^+ B^- - \overline{Re}^{-1}\partial_\zeta J^{-1}M(\zeta)] \Delta Q^n = \frac{\Delta Q^*}{J\Delta t}$$

$$RHS = \partial_\eta{}^- \hat{G}^+ + \partial_\eta{}^+ \hat{G}^- + \partial_\zeta{}^- \hat{H}^+ + \partial_\zeta{}^+ \hat{H}^-$$
$$-\overline{Re}^{-1}\partial_\zeta[J^{-1}(\zeta_x R + \zeta_y S)]$$

TURBULENCE MODEL: BALDWIN-LOMAX

BOUNDARY CONDITIONS: NO-SLIP, ADIABATIC WALL ON BODY

CHARACTERISTIC ANALYSIS IN FARFIELD

AIRFOIL GRID

This figure shows a partial view of a representative grid used in the airfoil calculations. It is a 193 x 65 C-mesh with clustering in the leading and trailing edge regions. Average minimum normal spacing on the body is 6.4×10^{-6} c. The grid extends 30 chords from the airfoil.

193 x 65 C-mesh
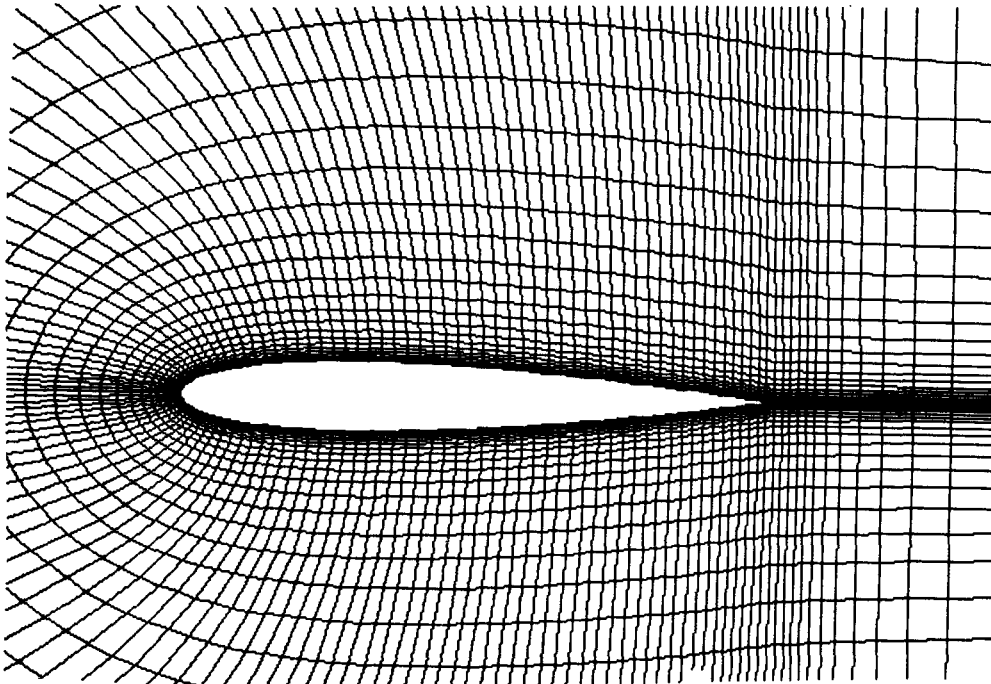
The NACA 0012 airfoil was analyzed at a Reynolds number of 3 million and a Mach number of 0.3 at several angles-of-attack up to and beyond stall. This figure shows computed lift coefficient versus angle-of-attack, alpha, in comparison with the experiments of Loftin and Smith[5] and Gregory and O'Reilly[6]. At 0, 10, and 15 deg., computed values are in excellent agreement with experimental results. At both 16 and 18 deg. angle-of-attack, within the region where experiment indicates stall accompanied by a sudden drop in lift, the computed flowfield is unsteady and periodic with lift coefficients varying in the ranges indicated in the figure. The maximum and minimum lift values agree well with the corresponding experimental values before and after stall, respectively. The Strouhal number of the periodic flow is given by St = $ncsin\alpha/u_\infty$, where n is the frequency of oscillation, c is the airfoil chord, α is the angle-of-attack, and u_∞ is the freestream flow velocity. At 21 deg., the periodic oscillation is no longer present. The results indicate a nearly steady solution, with only a small non-periodic variation in lift coefficient about an average value of about 1.05.

NACA 0012 airfoil, Re = 3 million
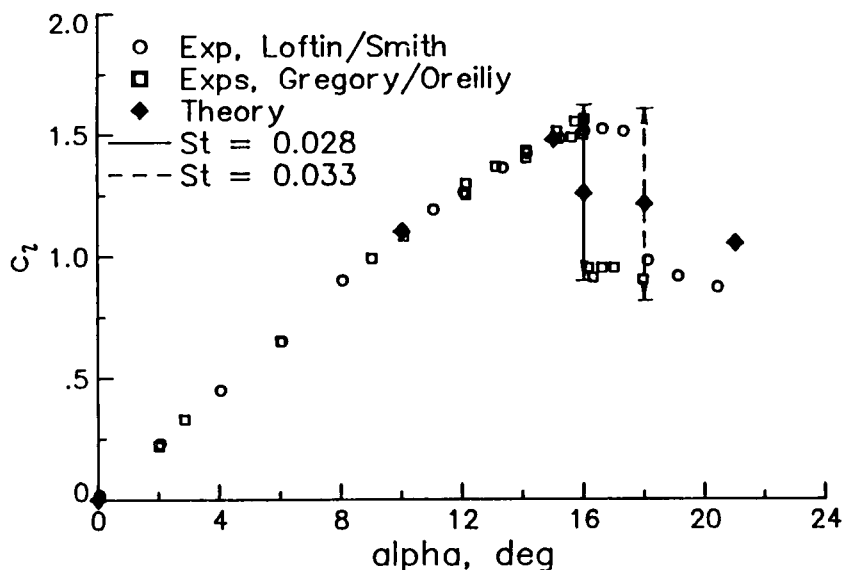
STEADY VORTICITY CONTOURS

Computed vorticity contours are shown for the NACA 0012 airfoil at 15 and 21 deg. angle-of-attack. At 15 deg., prior to stall onset, the vorticity is concentrated in a relatively thin-layer near the airfoil surface and behind the trailing edge. At 21 deg. the airfoil shows a region of massive separation above the airfoil upper surface. Vorticity levels are much higher than the 15 deg. case, with the strongest clockwise vorticity concentrated near the leading edge on the upper surface and the strongest counterclockwise vorticity again behind the trailing edge.

NACA 0012 airfoil, Re = 3 million

$\alpha = 15°$
$c_{\ell} = 1.48$

$\alpha = 21°$
$c_{\ell} = 1.05$
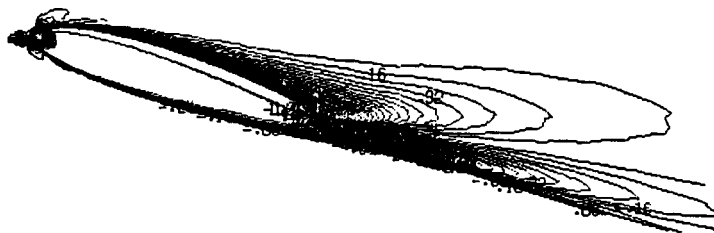
UNSTEADY VORTICITY CONTOURS

At 16 deg. angle-of-attack, the flowfield oscillates in a periodic manner, with the lift varying between a minimum of 0.89 and a maximum of 1.60. Vorticity contours are shown at four points in the unsteady periodic cycle. The cyclic nature of the flowfield is characterized by the shedding of a leading edge vortex near maximum lift.

NACA 0012 airfoil, Re = 3 million, α = 16°

c_ℓ = 1.60   max lift

c_ℓ = 0.89   min lift

c_ℓ = 1.31   decreasing

c_ℓ = 1.21   increasing
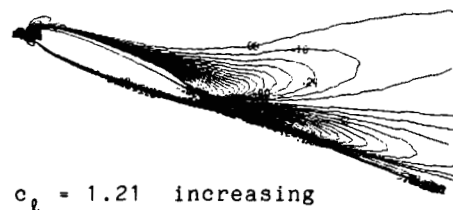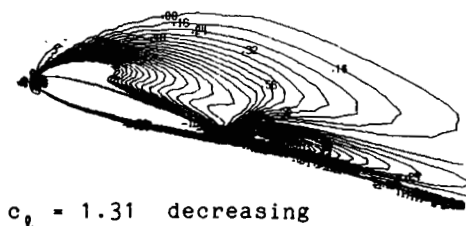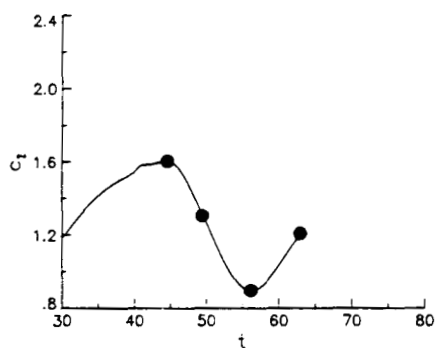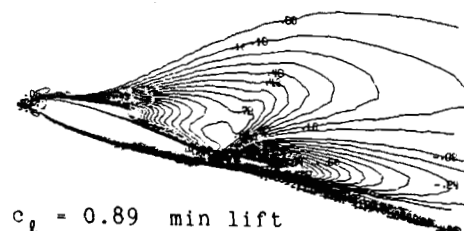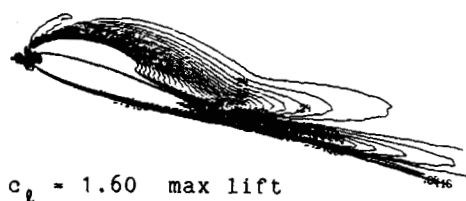
FORCED PITCHING SOLUTIONS

Computations have been performed in which the airfoil undergoes a forced pitching motion about its quarter chord. Two types of motion have been explored and results compared with experiment. The first is a sinusoidal pitching motion at high Reynolds number (turbulent flow) and the second is a constant-rate pitch from 0 to 60 deg. angle-of-attack at Re = 45,000 (laminar flow).

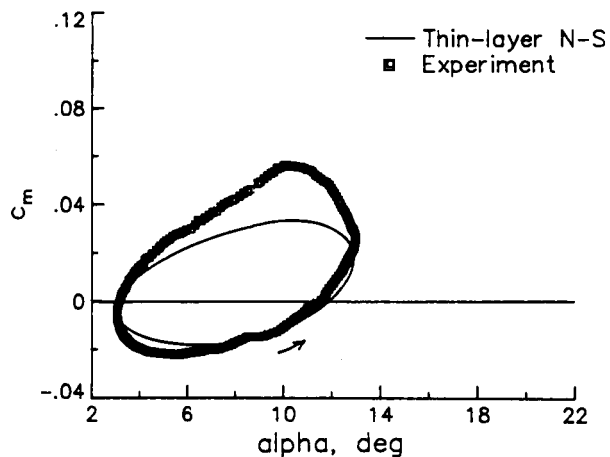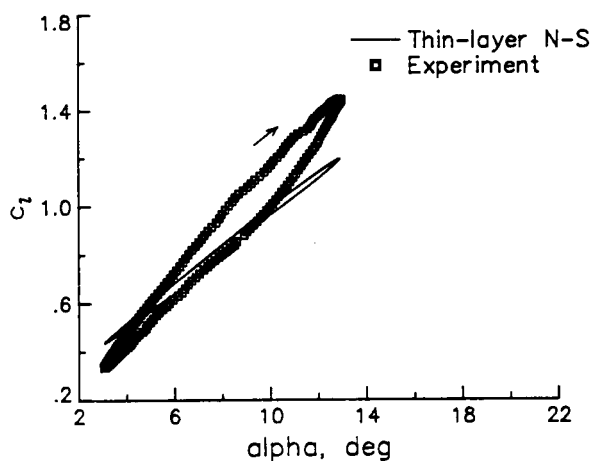$$\alpha(\tau) = \alpha_0 + \alpha_1 \sin(M_\infty k\tau) \qquad \text{sinusoidal pitch}$$

$$\alpha(\tau) = \alpha_0 + M_\infty k\tau \qquad \text{constant-rate pitch}$$

k = reduced frequency = $\omega c/u_\infty$
ω = frequency (rad/sec)
c = chord
u_∞ = freestream velocity
τ = time, nondimensionalized by c/a_∞
a_∞ = freestream speed of sound

The NACA 0012 airfoil was analyzed at Re = 3.89 x 10^6,
M = 0.301, α_0 = 7.97 deg., α_1 = 4.91 deg., and a reduced
frequency k = 0.398. This corresponds with Case 7111 from
McCroskey et al[7]. Transition to turbulence is fixed at the
leading edge in the computations but was not fixed in the
experiment. The time step taken for the computations is 0.05.
This figure shows the lift and moment coefficients as a function
of angle-of-attack. The thin-layer Navier-Stokes code predicts a
shallower lift versus alpha slope, slightly overpredicting the
minimum lift and underpredicting the maximum lift. Lift values
for increasing alpha are on the upper half of the lift curve for
both theory and experiment. The moment coefficient is in good
agreement with experiment when angle-of-attack is increasing
(lower half of the curve), but underpredicts the moment when
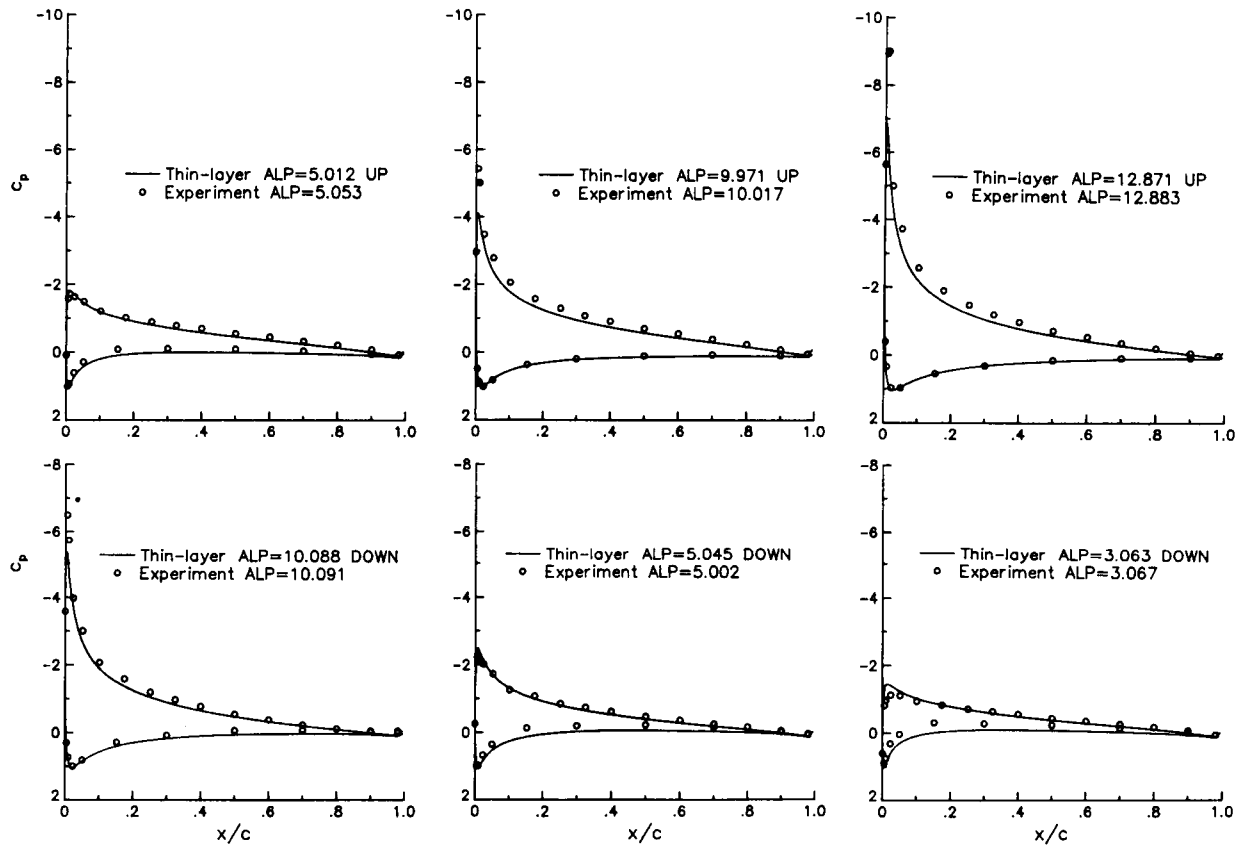angle-of-attack is decreasing.

NACA 0012 airfoil, Re - 3.89 x 10^6,
M - 0.301, α_0 - 7.97°, α_1 - 4.91°, k - 0.398

PRESSURE COEFFICIENTS

Pressure coefficients are compared with experiment at six times in the pitching cycle for Case 7111. Overall, the present method does well in predicting the shapes of the pressure curves.

NACA 0012 airfoil, $Re = 3.89 \times 10^6$, $M = 0.301$, $\alpha_0 = 7.97°$, $\alpha_1 = 4.91°$, $k = 0.398$

Thin-layer ALP=5.012 UP
Experiment ALP=5.053

Thin-layer ALP=9.971 UP
Experiment ALP=10.017

Thin-layer ALP=12.871 UP
Experiment ALP=12.883

Thin-layer ALP=10.088 DOWN
Experiment ALP=10.091

Thin-layer ALP=5.045 DOWN
Experiment ALP=5.002

Thin-layer ALP=3.063 DOWN
Experiment ALP=3.067

SINUSOIDAL PITCH SOLUTION WITH DEEP STALL

A solution with deep stall was computed at $Re = 3.76 \times 10^6$, $M = 0.292$, $\alpha_0 = 14.84$ deg., $\alpha_1 = 9.88$ deg., $k = 0.202$. These conditions correspond with Case 14210 from McCroskey et al[7]. In this case, both theory and experiment fixed transition to turbulence at the leading edge. Time step for the computations is 0.05. As seen from plots of lift and moment coefficient versus angle-of-attack, the computations agree well with experiment only as the angle-of-attack is increasing (upper portion of the lift curve, lower portion of the moment curve). However, theory predicts stall later than experiment. At all other points in the pitching cycle, theory and experiment are only qualitatively similar. Theory shows oscillations, which are not present in the experiment, in the lift and moment curves as the angle-of-attack decreases.

NACA 0012 airfoil, $Re = 3.76 \times 10^6$,
$M = 0.292$, $\alpha_0 = 14.84°$, $\alpha_1 = 9.88°$, $k = 0.202$
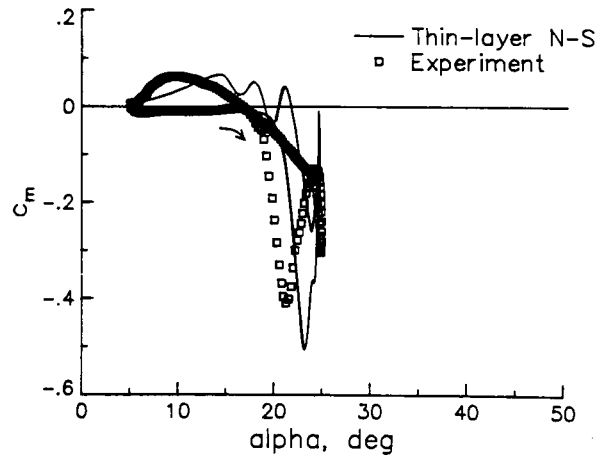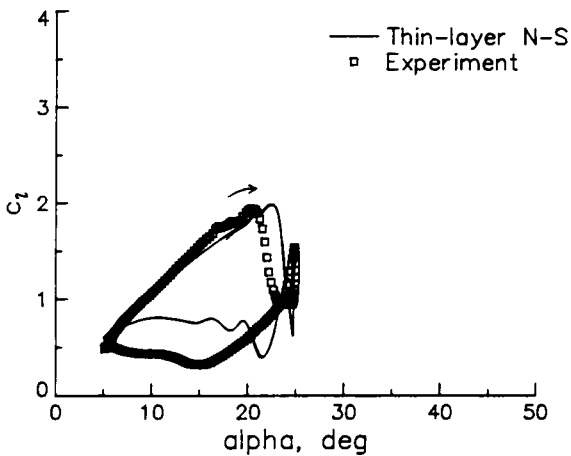
AGARD CASE SINUSOIDAL PITCH SOLUTIONS

Computations were performed to compare with two unsteady solutions from Landon[8]. The first, corresponding with AGARD Case 2, is at $Re = 4.8 \times 10^6$, $M = 0.6$, $\alpha_0 = 3.16$ deg., $\alpha_1 = 4.59$ deg., $k = 0.1622$. The second corresponds with AGARD Case 3: $Re = 4.8 \times 10^6$, $M = 0.6$, $\alpha_0 = 4.86$ deg., $\alpha_1 = 2.44$ deg., $k = 0.1620$. Lift and moment coefficients for each case are shown in the figure. In both cases, for theory and experiment, the lift values for increasing alpha are on the lower portion of the curve. The computations do fairly well to predict lift at the lower angles-of-attack but underpredict the lift at the high end of the cycles. Moment coefficients are underpredicted everywhere in the cycles, although for alpha increasing (lower portion of the curve) results are in closer agreement than for alpha decreasing. Results for Case 3 are very similar to those obtained by Howlett[9] using a small-disturbance potential code coupled with an inverse boundary-layer method. Howlett found that results near maximum lift are highly sensitive to the transition location. His results shown here have transition set at 20%. The thin-layer Navier-Stokes computations set transition at the leading edge, while experimental transition is unspecified.
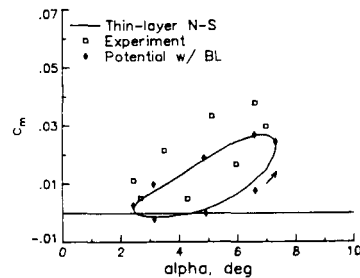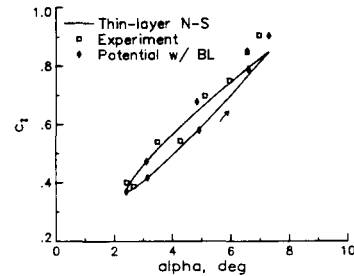
AGARD Case 2   AGARD Case 3

NACA 0012 airfoil, $Re = 4.8 \times 10^6$, $M = 0.6$
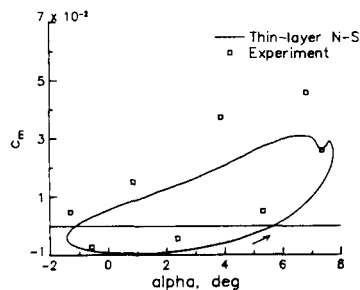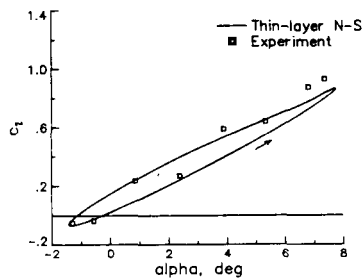
$\alpha_0 = 3.16°$, $\alpha_1 = 4.59°$, $k = 0.1622$ $\alpha_0 = 4.86°$, $\alpha_1 = 2.44°$, $k = 0.1620$

The real and imaginary components of lift and drag were computed for AGARD Cases 2 and 3 and compared with experiment. Agreement is fair, with the largest discrepancies in the imaginary component of moment for both cases. The values α_ℓ and α_m are the phase angles by which lift and moment cycles lead or lag the angle-of-attack cycle.

$$c_{\ell\alpha R} = \frac{2}{\alpha_1(t_2 - t_1)} \int_{t_1}^{t_2} [c_\ell(\tau) - c_{\ell avg}]\sin(M_\infty k\tau)\, d\tau$$

$$c_{\ell\alpha I} = \frac{2}{\alpha_1(t_2 - t_1)} \int_{t_1}^{t_2} [c_\ell(\tau) - c_{\ell avg}]\cos(M_\infty k\tau)\, d\tau$$

and similar expressions for $c_{m\alpha R}$ and $c_{m\alpha I}$

|	AGARD Case 2			AGARD Case 3		
	Exp	Theory	Error	Exp	Theory	Error
$c_{\ell\alpha R}$	6.616	5.67	14.3%	6.372	5.56	12.7%
$c_{\ell\alpha I}$	-0.891	-0.88	1.2%	-0.803	-0.75	6.6%
$c_{m\alpha R}$	0.224	0.172	23.2%	0.303	0.258	14.9%
$c_{m\alpha I}$	-0.244	-0.165	32.4%	-0.287	-0.200	30.3%
α_ℓ	-7.7°	-8.8°	14.3%	-7.2°	-7.7°	6.9%
α_m	-47.4°	-43.6°	8.0%	-43.4°	-37.8°	12.9%

CONSTANT-RATE PITCH SOLUTIONS, ω = 460 DEG/SEC

At a Reynolds number of 45,000, laminar flow computations of an NACA 0015 airfoil pitched up at a constant rate of 460 deg./sec (k = 0.2007) are compared with smoke wire flow visualizations of Helin and Walker[10]. Three angles-of-attack are shown in the figure. Flow is from right to left. With a time step of 0.05, computed velocity vectors show the same general trend as experiment, although the center of the shed leading-edge vortex does not convect downstream as quickly in the computations as it does in the experiment. At both 45 and 60 deg., there is reversed flow over most of the airfoil upper surface, due to the shed vortex.

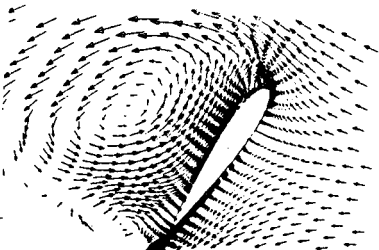NACA 0015 airfoil, Re = 45,000, laminar flow
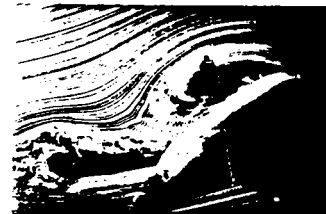ω = 460 deg./sec

COMPUTATION   EXPERIMENT


α = 30°

α = 45°

α = 60°
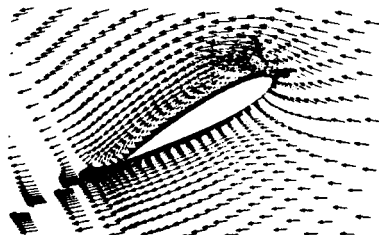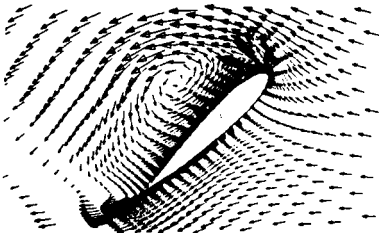
At a higher rate of pitch (k = 0.6021), computation with a time step of 0.02 shows a leading-edge vortex growth rate in good agreement with experiment. This vortex is much smaller in size than that for the lower pitch rate of 460 deg./sec. However, the computational analysis does not show the second region of separated flow near the trailing edge that is seen in the flow visualizations.
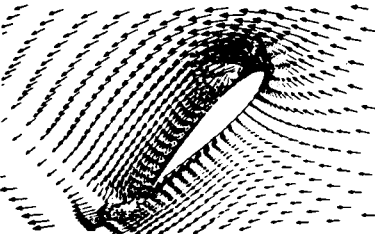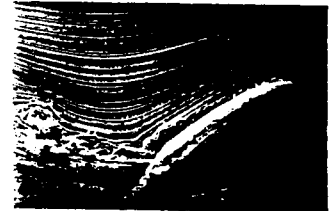
NACA 0015 airfoil, Re = 45,000, laminar flow

ω = 1380 deg./sec

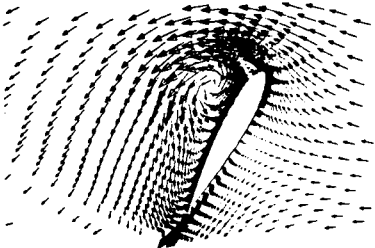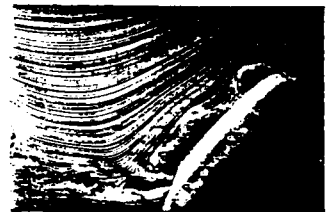COMPUTATION   EXPERIMENT

α = 30°

α = 45°
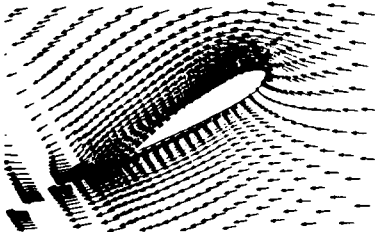
α = 60°
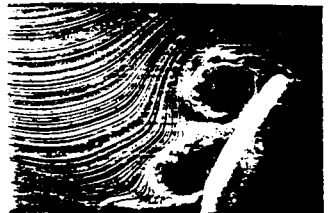
ORIGINAL PAGE IS OF POOR QUALITY

CONCLUSIONS

A finite volume implicit approximate factorization method which solves the thin-layer Navier-Stokes equations has been used to predict unsteady turbulent-flow airfoil behavior. At a constant angle-of-attack of 16 deg., the NACA 0012 airfoil exhibits an unsteady periodic flowfield with the lift coefficient oscillating between 0.89 and 1.60. The Strouhal number is 0.028. Results are similar at 18 deg., with a Strouhal number of 0.033. A leading-edge vortex is shed periodically near maximum lift.

Dynamic mesh solutions for unstalled airfoil flows show general agreement with experimental pressure coefficients. However, moment coefficients and the maximum lift value are underpredicted. The deep stall case shows some agreement with experiment for increasing angle-of-attack, but is only qualitatively comparable past stall and for decreasing angle-of-attack. Laminar-flow computations of a constant-rate pitch-up NACA 0015 airfoil show that increasing pitch rate slows separation. Computed velocity vectors agree qualitatively with experimental flow visualizations.

- CONSTANT ANGLE-OF-ATTACK

    - NACA 0012 FLOWFIELD UNSTEADY AT α = 16 AND 18 DEG.
        - lift oscillates within range of experiment
        - St = 0.03

    - PERIODICALLY SHED LEADING-EDGE VORTEX

- SINUSOIDAL PITCH

    - UNSTALLED CASES
        - pressure coefficients agree in general with experiment
        - moment coefficients and maximum lift underpredicted

    - DEEP STALL AGREES ONLY FOR α INCREASING

- CONSTANT-RATE PITCH

    - INCREASING PITCH RATE LESSENS SEPARATION

    - QUALITATIVE AGREEMENT WITH EXPERIMENT

REFERENCES

1.   Van Leer, B., "Flux-Vector Splitting for the Euler Equations," Lecture Notes in Physics, Vol. 170, 1982, pp. 501-512.

2.   Anderson, W., Thomas, J., and Rumsey, C., "Extension and Applications of Flux-Vector Splitting to Unsteady Calculations on Dynamic Meshes," AIAA Paper 87-1152-CP, 1987.

3.   Van Leer, B., "Towards the Ultimate Conservation Difference Scheme V. A Second Order Sequel to Gudonov's Method," Journal of Computational Physics, Vol. 32, 1979, pp. 101-136.

4.   Baldwin. B. and Lomax, H., "Thin Layer Approximation and Algebraic Model for Separated Turbulent Flows," AIAA Paper 78-257, 1978.

5.   Loftin, L., Jr. and Smith, H., "Aerodynamic Characteristics of 15 NACA Airfoil Sections at Seven Reynolds Numbers from 0.7×10^6 to 9.0×10^6," NACA TN 1945, 1949.

6.   Gregory, N. and O'Reilly, C., "Low-Speed Aerodynamic Characteristics of NACA 0012 Aerofoil Section, Including the Effects of Upper Surface Roughness Simulating Hoar Frost," NASA R&M 3726, 1970.

7.   McCroskey, W., McAlister, K., Carr, L., and Pucci, S., "An Experimental Study of Dynamic Stall on Advanced Airfoil Sections," NASA TM 84245, 1982.

8.   Landon, R., "NACA 0012. Oscillatory and Transient Pitching," Compendium of Unsteady Aerodynamic Measurement, AGARD-R-702.

9.   Howlett, J., "Viscous Flow Calculations for the AGARD Standard Configuration Airfoils with Experimental Comparisons," Langley Symposium on Transonic Unsteady Aerodynamics and Elasticity, 1987, NASA CP 3022, pp. 313- 350.

10.   Helin, H. and Walker, J., "Interrelated Effects of Pitch Rate and Pivot Point on Airfoil Dynamic Stall," AIAA Paper 85-0130, 1985.